



Article submitted to journal

Subject Areas:

Electromagnetism, Computer modelling and simulation, Applied mathematics

Keywords:

Homogenization, Ferroelectrics, Metamaterials , Tunability

Author for correspondence:

Benjamin Vial

e-mail: b.vial@qmul.ac.uk

Homogenization of periodic and random ferroelectric-dielectric composites

Benjamin Vial and Yang Hao

School of Engineering and Computer Science, Queen Mary, University of London, London, E1 4NS, United Kingdom

We investigate the homogenized permittivity of ferroelectric-dielectric mixtures under a static electric field. A refined model is used to take into account the coupling between the electrostatic problem and the electric field dependent permittivity of the ferroelectric material. Periodic and random structures in two dimensions are investigated and we study the effective permittivity, losses, electrically induced anisotropy and tunability of those metamaterials.

1. Introduction

Ferroelectric materials play a crucial role in reconfigurable microwave devices, with typical applications including antenna beam steering, phase shifters, tunable power splitters, filters, voltage controlled oscillators and matching networks [1]. Both bulk ceramics and thin films have been employed to design frequency agile components [2–4] and metamaterials [5,6]. The main reason of using ferroelectric materials is their strong dependence of their permittivity ε on an applied electric field E , which is measured by their tunability defined as $n = \varepsilon(0)/\varepsilon(E)$. The key requirements for antenna and microwave applications are large tunability and low losses. These two characteristics are correlated and one has to find a trade-off for optimal device performance, which can be quantified by the so called commutation quality factor $K = (n - 1)^2 / (n \tan \delta(0) \tan \delta(E))$, where $\tan \delta$ is the loss tangent.

These materials have usually high permittivity values, often leading to slow response time and impedance mismatch, which can be an issue in some practical applications. Thus it has been considered to mix ferroelectric ceramics to low-index and low-loss non-tunable dielectrics in order to reduce both permittivity

values and losses. The effective parameters of those composites have been investigated [7–10] and it has been found that the permittivity can be greatly reduced while losses are much less sensitive to the dielectric phase addition, and in some situations lead to a small increase of the tunability of the mixture. In the context of porous ferroelectrics, the homogenized properties strongly depends on the size and morphology of the pores [11,12]. In addition, the influence of local field enhancement in the tunability has been shown to be of particular importance [13–15]. This study investigates the effective permittivity of composites made of dielectric inclusions in a ferroelectric matrix by using a two-scale convergence method [16,17]. The originality lies in the fact that a fully coupling model is employed to calculate the electrostatic field distribution when a uniform biasing field is applied on the structures, which will result in a local modification of the permittivity in the ferroelectric phase due to the microstructure. As compared to a simple uncoupled model where the ferroelectric phase is only modified through the biasing field, the resulting effective permittivity, dielectric losses, tunability and anisotropy significantly differ. As compared to earlier studies in the literature [13,14], we account for the non-linear coupling beyond the first iteration and use two-scale convergence homogenization analysis to obtain the effective parameters at higher frequencies, instead of a capacitance-based model. We first study metamaterials consisting of a square array of parallel dielectric rods with circular cross section in a ferroelectric host, and then investigate the effect of random distribution of those rods within the unit cell.

2. Theory and numerical model

We consider a composite made of a ferroelectric material with anisotropic permittivity $\epsilon^f(\mathbf{E})$ that is dependent on an applied electric field \mathbf{E} , and a non tunable dielectric of permittivity ϵ^d , which are both non-magnetic. The structures under study are invariant along the z direction, which leads to the standard decomposition of the wave equation in the transverse electric case (TE, electric field parallel to the direction of invariance) and the transverse magnetic case (TM, magnetic field parallel to the direction of invariance). A uniform biasing field is applied in order to be able to tune the effective permittivity. Modelling homogenized properties of this type of mixtures can be done by assuming that the electric field distribution is uniform throughout the sample, so that the study of the tunability is essentially achieved by changing the value of the properties in the ferroelectric phase and computing the effective permittivity of the composite. We refer this approach as to the uncoupled model in the following. However, a more accurate description is to take into account the change of the electric field by the microstructure, if any. We therefore need to solve an electrostatic equation to find the field distribution within the material, but its solution depends on the permittivities of both materials, and the permittivity in the ferroelectric phase depends on this induced electric field: this leads to a strongly coupled problem.

(a) Permittivity model

We use barium strontium titanate (BST) as our ferroelectric material. Measurements have been carried out at electrostatics and at microwave frequencies, and the normalized permittivity value as a function of biasing field are reported on Fig. (1).

To describe the permittivity, we make use of the Landau potential given by $F(P, E) = F_0 + aP^2/2 + bP^4/4 + cP^6/6 - EP$, where E is the applied electric field and P is the polarization [18,19]. Variations of the permittivity with the temperature can be taken into account through the coefficients a , b and c , but we assume we are working at a constant room temperature. We further assume that the material is not subject to any stress, so that the variation of permittivity due to mechanical constraints is irrelevant. The equation of state

$$\frac{\partial F(P, E)}{\partial P} = aP_0 + bP_0^3 + cP_0^5 - E = 0$$

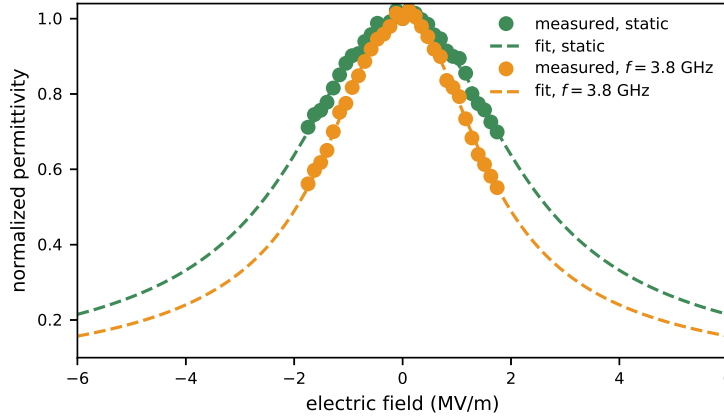


Figure 1. Variation of the ferroelectric permittivity as a function of the applied electric field (dots: measurements, dashed lines: fit to formula (2.1)), for the static case (green) and at microwave frequencies (orange, $f = 3.8$ GHz). The fitting parameters are given in Table 1.

Table 1. Fitting parameters to model (2.1) for the measured permittivity values as a function of applied electric field shown on Fig. (1).

case	$\varepsilon^f(0)$	$\alpha (\mu\text{m}^2/\text{V}^2)$	$\beta (\mu\text{m}^4/\text{V}^4)$
static	3050	0.120	0.024
$f = 3.8$ GHz	165	0.240	0.079

gives the dependence of the polarization on the applied electric field, with P_0 being the equilibrium polarization. Along the direction of a uniform applied electric field, the relative permittivity is given by:

$$\varepsilon^f(E) = \left[\frac{\partial^2 F(P, E)}{\partial P^2} \right]^{-1} = \frac{\varepsilon^f(0)}{1 + \alpha P_0^2 + \beta P_0^4}, \quad (2.1)$$

where $\varepsilon^f(0) = 1/a$, $\alpha = 3b/a$ and $\beta = 5c/a$. The fitting parameters are given in Table 1. As the norm of the field increases, the permittivity decreases with a characteristic bell curve typical for a ferroelectric material in its paraelectric state. Furthermore, assuming the crystalline principal axes of the ferroelectric material are oriented in the coordinate directions, and that the diagonal components of the permittivity tensor are only function of the corresponding bias electric field components [20], we have:

$$\boldsymbol{\varepsilon}^f(\mathbf{E}) = \begin{pmatrix} \varepsilon_{xx}^f(E_x) & 0 & 0 \\ 0 & \varepsilon_{yy}^f(E_y) & 0 \\ 0 & 0 & \varepsilon_{zz}^f(E_z) \end{pmatrix} \quad (2.2)$$

where each of the diagonal components have the functional form given by Eq. (2.1). Note that we will use the static values of permittivity for the electrostatic modelling, while we are interested in the homogenized values of permittivity at microwaves.

(b) Electrostatic model

The composites under study are made of two materials, thus their permittivity is represented by a piecewise defined tensor $\epsilon(\mathbf{r}, \mathbf{E})$ which is equal to $\epsilon^f(\mathbf{E}(\mathbf{r}))$ in the ferroelectric phase and $\text{diag}(\epsilon^d)$ in the dielectric phase. In the following, we consider two different cases for the biasing field. Because of the form (2.2) assumed for the ferroelectric permittivity tensor, ϵ_{zz} will not be changing for a field in the plane orthogonal to the z axis. This is the only component being relevant for TE polarization, so we consider in this case a uniform biasing electric field applied along the direction of invariance $\mathbf{E}_0 = E_0 \mathbf{e}_z$. On the other hand, the in-plane components of ϵ^f are tuned by E_x and E_y , therefore, without loss of generality, we consider a uniform applied electric field directed along the x axis $\mathbf{E}_0 = E_0 \mathbf{e}_x$ for the TM polarization case. To calculate the total electric field in the material, one has to solve the electrostatic equation for the potential V :

$$\nabla \cdot (\epsilon \nabla V) = 0 \quad (2.3)$$

Note that for the TE case, the solution is trivial since the structures are invariant along z , so that the electric field is equal to the uniform biasing field, and we will thus not study it in the following. However in the TM case, the situation is much more complex: this is a coupled problem since the electric field $\mathbf{E} = -\nabla V$ derived from the solution of Eq. (2.3) depends on the permittivity distribution, which itself depends on the electric field. The coupled system formed of Eqs. (2.2) and (2.3) is solved iteratively until there is convergence on the norm of the electric field. Here we would like to emphasise that the permittivity in the ferroelectric material, although uniform initially, is spatially varying due to the non-uniform distribution of the total electric field.

(c) Homogenization

The effective permittivity for TM polarization is calculated using two scale homogenization technique [16,17]. For this purpose, one has to find the solutions ψ_j of two annex problems \mathcal{P}_j , $j = \{1, 2\}$:

$$\nabla \cdot [\xi \nabla (\psi_j + r_j)] = 0, \quad (2.4)$$

where $\mathbf{r} = (x, y)^T$ is the position vector in the xy plane and $\xi = \epsilon^T / \det(\epsilon)$. The homogenized tensor $\tilde{\xi}$ is obtained with:

$$\tilde{\xi} = \langle \xi \rangle + \phi, \quad (2.5)$$

where $\langle \cdot \rangle$ denotes the mean value over the unit cell. The elements of the matrix ϕ represent correction terms and are given by $\phi_{ij} = \langle \xi \nabla \psi_i \rangle_j$. Finally the effective permittivity tensor can be calculated using $\tilde{\epsilon} = \tilde{\xi}^T / \det(\tilde{\xi})$.

Note that the TE case, which we shall not study here as no coupling happens, is trivial since the homogenized permittivity is simply the average of the permittivity in the unit cell: $\tilde{\epsilon} = \langle \epsilon \rangle$.

(d) Numerical setup

Equations (2.3) and (2.4) are solved with a Finite Element Method using the open source packages Gmsh [21] and GetDP [22]. In both cases we use a square unit cell Ω of length d with periodic boundary conditions along x and y . Second order Lagrange elements are used and the solution is computed with a direct solver (MUMPS [23]).

3. Numerical results

In the following numerical results, the dielectric phase is supposed to be lossless and non dispersive with $\epsilon^d = 3$ while the ferroelectric material follows the permittivity described in section (a) and has a constant loss tangent $\tan \delta^f = 10^{-2}$.

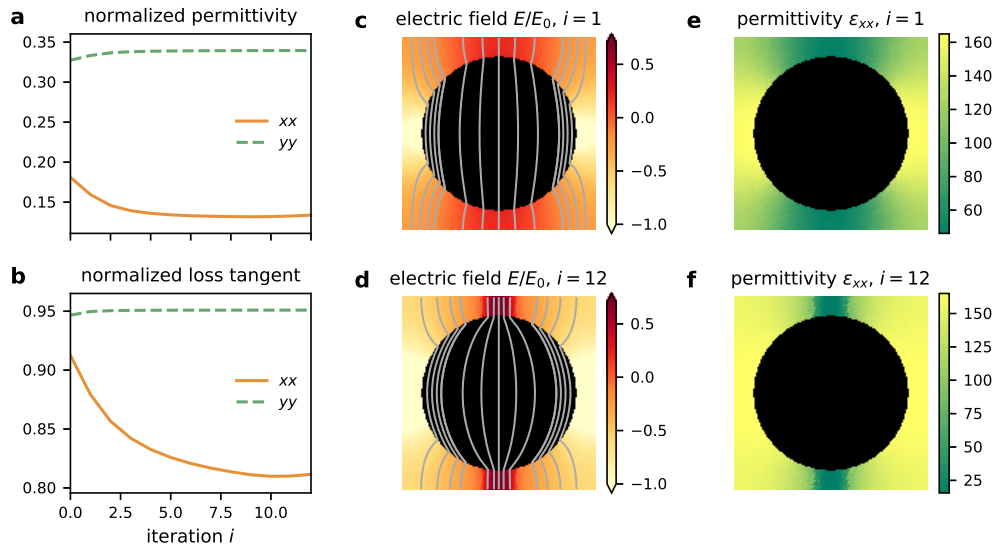


Figure 2. Convergence of the coupled problem. Real part (a) and loss tangent (b) of the components of the homogenized permittivity tensor as a function of iteration step i . The distribution of the normalized electric field (colour map: magnitude in logarithmic scale, lines: equipotential contours) and of the xx component of the permittivity tensor are shown for $i = 1$ (c and d) and $i = 12$ (e and f).

(a) Two dimensional periodic metamaterial

Lets us now consider a periodic square array of infinitely long dielectric rods of circular cross section of radius r embedded in a ferroelectric matrix.

We first study the convergence of the coupled problem on the particular case with dielectric filling fraction $f = \pi r^2/d^2 = 0.5$ and $E_0 = 2\text{MV/m}$. Figures 2(a) and 2(b) show the convergence of the real part and loss tangent of the components of the homogenized permittivity tensor, respectively. The yy components converge quickly and are almost unaffected by the coupling process whereas the xx components change substantially from the initial conditions. This is due to the effect of the redistribution of the electrostatic field within the unit cell (see Figs. (2.c) and (2.d)), where the x component of the electric field is still much stronger than the y component, even if spatially varying in the ferroelectric medium. At equilibrium, the electric field is concentrated close to the y axis in between two neighbouring rods. This in turn affects the permittivity distribution (see Figs. (2.e) and (2.f)), and the homogenized properties of the composite.

We computed the effective parameters of these metamaterial structures for different radii of the rods and studied their behaviour when subjected to an external electrostatic field (see Fig. (3)). The results of our coupled model differ significantly from the uncoupled one. Increasing the dielectric fraction lowers the effective permittivity while the losses are slightly reduced but much less sensitive. Due to the inhomogeneous redistribution of the permittivity over the ferroelectric domain, the overall tunability changes. In the case studied here, taking into account the coupling leads to an effective tunability increase with higher dielectric concentration, and that is larger than the tunability of bulk ferroelectric. Two concurrent effects are at stake here: on the one hand the dilution of ferroelectric makes the composite less tunable, but on the other hand, the rearrangement of the electrostatic field surrounding the inclusion and its concentration in some region will cause a higher permittivity change locally. The relative strength of those phenomena is governed by the shape of the inclusion and its permittivity and so it is envisioned that the performance of the composites might be enhanced by engineering their microstructure. The geometry of the unit cell is symmetric so the homogenized material is isotropic when no field

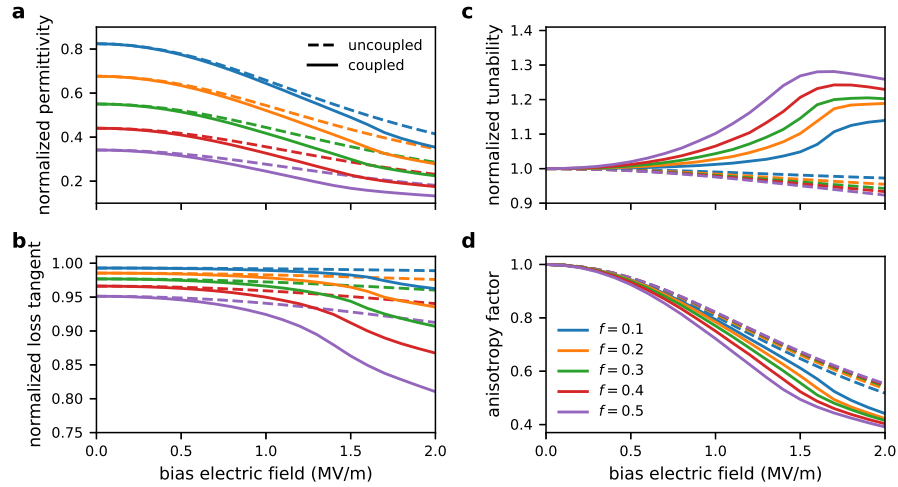


Figure 3. Effective parameters of the 2D metamaterials as a function of the applied electric field for various filling fraction of dielectric. (a): normalized permittivity, (b): normalized loss tangent, (c): normalized tunability and (d): anisotropy factor. The solid lines correspond to the coupled model and the dashed lines to the uncoupled model.

is applied. But when the sample is biased, the permittivity distribution becomes asymmetric due to the inhomogeneity of the electric field, thus making the effective material properties anisotropic. This geometric effect is added to the anisotropy arising from the material properties of the ferroelectric phase itself, and depending on the topology and permittivity of the rods, one effect would be predominant. In the case studied here, the equilibrium permittivity distribution varies strongly along the bias direction and much less orthogonally to it, which adds anisotropy by diminishing the effective permittivity in the x direction. This is local field induced effect is what makes the anisotropy stronger in our coupled model compared to the uncoupled one (cf. Fig. (3.d)). Those subtle phenomena can only be rigorously taken into account by employing a coupling formalism and are responsible for the difference observed when compared to a simple uncoupled model.

(b) Random case

We finally study the effect of random particle distribution on the effective parameters of the composites. This is an important point as fabrication of randomly dispersed inclusions is much more easy from a technological perspective. For each filling fraction of the dielectric, we generated 21 numerical samples with inclusions of circular cross section of average radius $r = d/20$ that can vary by $\pm 30\%$. Their centre is chosen randomly and the rods are allowed to overlap. An example of distribution for $f = 0.5$ is given on Fig. (6). The effective material properties are plotted on Fig. (4). Similarly to the periodic case, the permittivity decreases with increasing dilution of ferroelectric, but for identical filling fraction, the permittivity is lower as compared to the periodic array, and the smaller the dielectric concentration the larger is the difference. Losses decrease as well and the reduction is substantially larger than the periodic case, with higher variation from sample to sample as f increases. The effective tunability is on average smaller than that in the periodic case, and for low biasing fields and for some particular samples can be greater than the bulk tunability. However, at higher applied electric fields, normalized tunability becomes smaller than unity and is reduced as one adds more dielectric. For comparison, the homogenized parameters are plotted on Fig. (7) in the case where the coupling is neglected. One can see that

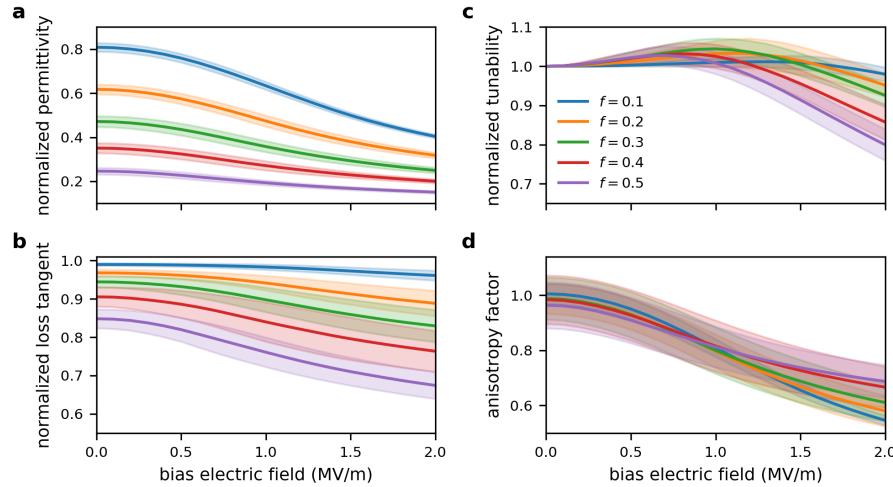


Figure 4. Effective parameters of the random 2D mixtures as a function of the applied electric field for various filling fraction of dielectric, when the coupling is taken into account. (a): normalized permittivity, (b): normalized loss tangent, (c): normalized tunability and (d): anisotropy factor. The solid lines represent the average values over the 21 samples and the lighter error bands show a confidence interval corresponding to the standard deviation.

the coupled and uncoupled models give similar results for the tunability whereas the losses are still smaller for the coupled case at higher fields.

The redistribution of electric field, permittivity and convergence of the effective parameters are displayed in Fig. (5). The effect of disorder plays an important role here: the electrostatic field gets concentrated in between neighbouring inclusions and the smaller the gap the higher the field, hence a greater local permittivity change. In addition, even if the distribution of particle is random, one expects that the anisotropy due to geometry would cancel for a sufficiently large number of particles (which is the case as the mean anisotropy factor is close to 1 when no bias field is applied). However, the anisotropy due to ferroelectric properties is important in this case as well, as both the x and y components of the electrostatic field are playing a role. Because of the relative positions of the rods, both ε_{xx} and ε_{yy} are affected by the coupling, so that the anisotropy factor for higher fields is reduced as compared to the periodic case. However even if there is a substantial variability from sample to sample, on average, the anisotropy factor decreases with increasing dielectric concentration.

4. Conclusion

We have studied the homogenized properties of dielectric/ferroelectric mixtures using a rigorous model that take into account the coupling between the electrostatic field distribution and the field dependant ferroelectric permittivity tensor. After convergence of the coupled problem, the effective permittivity tensor is calculated using two scale convergence homogenization theory. The results obtained by this model differ significantly from a simple assumption that the permittivity of the ferroelectric respond just to the uniform biasing field. We have considered both periodic and random arrays of dielectric rods in a ferroelectric matrix in 2D, and studied their effective properties for TM polarization as a function of dielectric concentration and bias field. Importantly, adding more low index and low loss dielectric allows to decrease the overall permittivity significantly and slightly lower the losses. For the periodic case, the tunability is higher than the bulk due to local field enhancement, whereas this effect is strongly suppressed when disorder is introduced. The assymetric redistribution of the permittivity induce en effective

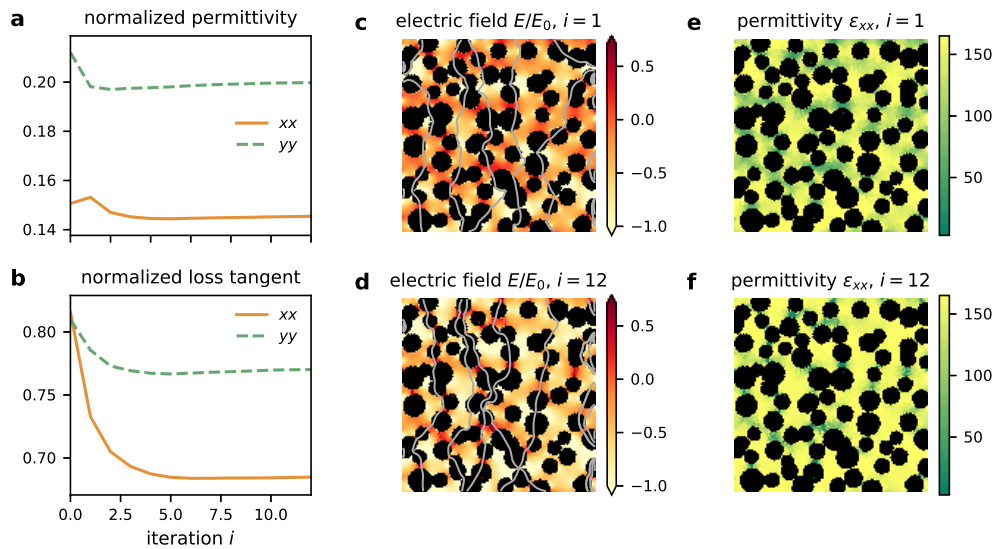


Figure 5. Convergence of the coupled problem in the random case for one sample. Real part (a) and loss tangent (b) of the components of the homogenized permittivity tensor as a function of iteration step i . The distribution of the normalized electric field (colour map: magnitude in logarithmic scale, lines: equipotential contours) and of the xx component of the permittivity tensor are shown for $i = 1$ (c and d) and $i = 12$ (e and f).

anisotropy that is added to the one arising purely from the ferroelectric material. The properties of the composites are affected by multiple factors: geometry and the spatially dependent electric field that will induce locally a tunable, anisotropic response in the ferroelectric phase depending on its amplitude and direction. This suggests that the performances of the composites may be enhanced by distributing the two phases in an optimal way to get high tunability and low losses. Further work in that direction is needed as well as extending this study to 3D media. Finally, because the permittivity of the dielectric is much smaller than the ferroelectric one, it would be of great interest to use high contrast homogenization theory [24,25] to study this kind of mixtures. This would reveal the frequency dependant artificial magnetism due to "micro-resonances" in the high index phase and potentially lead to composites with tunable effective permeability.

A. Random permittivity distribution and uncoupled effective parameters

Data Accessibility. The codes necessary to reproduce the results in this article are freely available at github.com/benvial/ferromtm.

Authors' Contributions. Benjamin Vial wrote devised the research, implemented the codes and wrote the paper. Yang Hao supervised the research and co-authored the manuscript.

Competing Interests. The authors declare no competing interests.

Funding. This work was funded by the Engineering and Physical Sciences Research Council (EPSRC), UK, under a grant (EP/P005578/1) 'Adaptive Tools for Electromagnetics and Materials Modelling to Bridge the Gap between Design and Manufacturing (AOTOMAT)'.

Acknowledgements. The authors would like to thank Henry Giddens for performing the measurements of ferroelectric permittivity used in this paper.

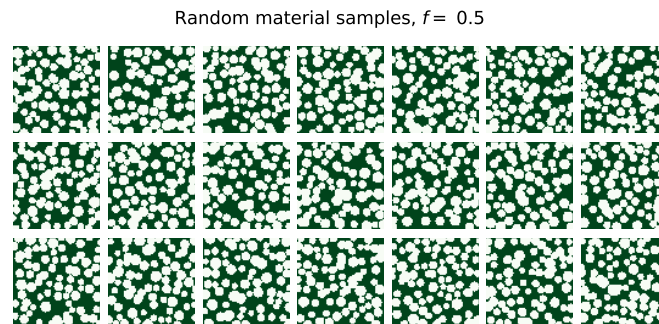


Figure 6. Permittivity distribution of the numerical samples used for $f = 0.5$. Dark colour indicates the ferroelectric material while light colour represents the dielectric inclusions.

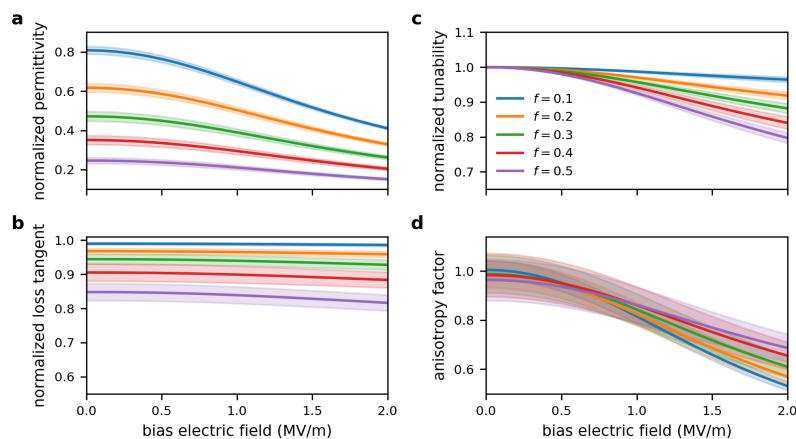


Figure 7. Effective parameters of the random 2D mixtures as a function of the applied electric field for various filling fraction of dielectric, when the coupling is neglected. (a): normalized permittivity, (b): normalized loss tangent, (c): normalized tunability and (d): anisotropy factor. The solid lines represent the average values over the 21 samples and the lighter error bands show a confidence interval corresponding to the standard deviation.

References

1. Tagantsev AK, Sherman VO, Astafiev KF, Venkatesh J, Setter N. 2018 Ferroelectric Materials for Microwave Tunable Applications. *J. Electroceram.* **11**, 5–66.
2. Vendik O, Hollmann E, Kozyrev A, Prudan A. 1999 Ferroelectric tuning of planar and bulk microwave devices. *Journal of Superconductivity* **12**, 325–338.
3. Lancaster M, Powell J, Porch A. 1998 Thin-film ferroelectric microwave devices. *Superconductor Science and Technology* **11**, 1323.
4. Xi X, Li HC, Si W, Sirenko A, Akimov I, Fox J, Clark A, Hao J. 2000 Oxide thin films for tunable microwave devices. *Journal of Electroceramics* **4**, 393–405.
5. Hand TH, Cummer SA. 2008 Frequency tunable electromagnetic metamaterial using ferroelectric loaded split rings. *Journal of Applied Physics* **103**, 066105.
6. Zhao H, Kang L, Zhou J, Zhao Q, Li L, Peng L, Bai Y. 2008 Experimental demonstration of tunable negative phase velocity and negative refraction in a ferromagnetic/ferroelectric composite metamaterial. *Applied Physics Letters* **93**, 201106.
7. Sherman VO, Tagantsev AK, Setter N, Iddles D, Price T. 2006 Ferroelectric-dielectric tunable composites. *Journal of Applied Physics* **99**, 074104.

8. Jylha L, Sihvola AH. 2008 Tunability of granular ferroelectric dielectric composites. *Progress in Electromagnetics Research* **78**, 189–207.
9. Sherman VO, Tagantsev AK, Setter N. 2004 Tunability and loss of the ferroelectric-dielectric composites. In *14th IEEE International Symposium on Applications of Ferroelectrics, 2004. ISAF-04*. 2004 pp. 33–38.
10. Astafiev KF, Sherman VO, Tagantsev AK, Setter N. 2003 Can the addition of a dielectric improve the figure of merit of a tunable material?. *Journal of the European Ceramic Society* **23**, 2381 – 2386.
11. Okazaki K, Nagata K. 1973 Effects of Grain Size and Porosity on Electrical and Optical Properties of PLZT Ceramics. *Journal of the American Ceramic Society* **56**, 82–86.
12. Stanculescu R, Ciomaga CE, Padurariu L, Galizia P, Horchidan N, Capiani C, Galassi C, Mitoseriu L. 2015 Study of the role of porosity on the functional properties of (Ba,Sr)TiO₃ ceramics. *Journal of Alloys and Compounds* **643**, 79–87.
13. Padurariu L, Curecheriu L, Galassi C, Mitoseriu L. 2012a Tailoring non-linear dielectric properties by local field engineering in anisotropic porous ferroelectric structures. *Appl. Phys. Lett.* **100**, 252905.
14. Padurariu L, Curecheriu L, Buscaglia V, Mitoseriu L. 2012b Field-dependent permittivity in nanostructured BaTiO₃ ceramics: Modeling and experimental verification. *Phys. Rev. B* **85**, 224111.
15. Cazacu A, Curecheriu L, Neagu A, Padurariu L, Cernescu A, Lisiecki I, Mitoseriu L. 2013 Tunable gold-chitosan nanocomposites by local field engineering. *Appl. Phys. Lett.* **102**, 222903.
16. Allaire G. 1992 Homogenization and Two-Scale Convergence. *SIAM Journal on Mathematical Analysis* **23**, 1482–1518.
17. Guenneau S, Zolla F. 2000 Homogenization of Three-Dimensional Finite Photonic Crystals. *Journal of Electromagnetic Waves and Applications* **14**, 529–530.
18. Landau LD, Bell J, Kearsley M, Pitaevskii L, Lifshitz E, Sykes J. 2013 *Electrodynamics of continuous media* vol. 8. elsevier.
19. Zhou K, Boggs SA, Ramprasad R, Aindow M, Erkey C, Alpay SP. 2008 Dielectric response and tunability of a dielectric-paraelectric composite. *Applied Physics Letters* **93**, 102908.
20. Krowne CM, Daniel M, Kirchoefer SW, Pond JA. 2002 Anisotropic permittivity and attenuation extraction from propagation constant measurements using an anisotropic full-wave Green's function solver for coplanar ferroelectric thin-film devices. *IEEE Transactions on Microwave Theory and Techniques* **50**, 537–548.
21. Geuzaine C, Remacle JF. 2009 Gmsh: A 3-D finite element mesh generator with built-in pre- and post-processing facilities. *International Journal for Numerical Methods in Engineering* **79**, 1309–1331.
22. Dular P, Geuzaine C, Henrotte F, Legros W. 1998 A general environment for the treatment of discrete problems and its application to the finite element method. *IEEE Transactions on Magnetism* **34**, 3395–3398.
23. Amestoy PR, Duff IS, Koster J, L'Excellent JY. 2001 A Fully Asynchronous Multifrontal Solver Using Distributed Dynamic Scheduling. *SIAM Journal on Matrix Analysis and Applications* **23**, 15–41.
24. Bouchitté G, Felbacq D. 2004 Homogenization near resonances and artificial magnetism from dielectrics. *Comptes Rendus Mathématique* **339**, 377 – 382.
25. Cherednichenko K, Cooper S. 2015 Homogenization of the system of high-contrast Maxwell equations. *Mathematika* **61**, 475–500.